








Responsibility of major emitters for country-level warming and extreme hot years

Lea Beusch ¹, Alexander Nauels ^{2,3}, Lukas Gudmundsson ¹, Johannes Gütschow ⁴, Carl-Friedrich Schleussner ^{2,5} & Sonia I. Seneviratne ¹

The contributions of single greenhouse gas emitters to country-level climate change are generally not disentangled, despite their relevance for climate policy and litigation. Here, we quantify the contributions of the five largest emitters (China, US, EU-27, India, and Russia) to projected 2030 country-level warming and extreme hot years with respect to pre-industrial climate using an innovative suite of Earth System Model emulators. We find that under current pledges, their cumulated 1991–2030 emissions are expected to result in extreme hot years every second year by 2030 in twice as many countries (92%) as without their influence (46%). If all world nations shared the same fossil CO₂ per capita emissions as projected for the US from 2016–2030, global warming in 2030 would be 0.4 °C higher than under actual current pledges, and 75% of all countries would exceed 2 °C of regional warming instead of 11%. Our results highlight the responsibility of individual emitters in driving regional climate change and provide additional angles for the climate policy discourse.

¹Institute for Atmospheric and Climate Science, ETH Zurich, Zurich, Switzerland. ²Climate Analytics, Berlin, Germany. ³Australian-German Climate & Energy College, University of Melbourne, Parkville, Australia. ⁴Potsdam Institute for Climate Impact Research, Member of the Leibniz Association, Potsdam, Germany. ⁵IRI THESys and Geography Faculty, Humboldt-Universität zu Berlin, Berlin, Germany. ✉email: lea.beusch@env.ethz.ch

It has been known for over a century that human-induced greenhouse gas (GHG) emissions lead to a warming planet^{1–3}. In 1990, with the first assessment report of the Intergovernmental Panel on Climate Change (IPCC)⁴, the scientific community presented for the first time a comprehensive review on the state of knowledge on climate change to policy-makers and the public. Several IPCC reports later, in 2015, the world's nations came together under the Paris Agreement and agreed to aim at “holding the increase in the global average temperature to well below 2 °C above pre-industrial levels and to pursue efforts to limit the temperature increase to 1.5 °C above pre-industrial levels”⁵. As part of the Paris Agreement, each country must plan, communicate, and implement Nationally Determined Contributions (NDCs) to reduce its emissions. The current round of NDCs covers the time horizon up to 2030.

Evidence of human influence on the climate system is ever increasing, but classical attribution science is generally based solely on global-scale emissions^{6–8}. Recent studies have highlighted the relevance of assigning climate change responsibility to major emitters^{9–15}, in order to better quantify the contributions of individual countries to human-induced global warming and its consequences. This has gained importance with the bottom-up approach to mitigation that was introduced as part of the Paris Agreement, in which each country decides its own mitigation efforts without international negotiations. However, no study so far has assessed implications for regional climate change in single countries and in the context of combined historical and currently pledged near-term future emissions.

Here, we use a chain of Earth System Model (ESM) emulators to translate historical emissions and currently pledged NDCs (as of September 2021) into projected regional climate changes until 2030. The focus is set on the contributions of the top five largest emitters—China, the United States (US), the European Union (EU-27), India, and Russia—to country-level warming and extreme hot years with respect to pre-industrial climate (1850–1900) over two time periods: (1) the time period during which policy-makers have been informed about the looming climate crisis by the IPCC (1991–2030, henceforth the IPCC period), and (2) the time period after the Paris Agreement was reached (2016–2030, henceforth the Paris period). As an additional climate change responsibility perspective, emission scenarios are explored in which global per capita emissions of the dominant GHG fossil CO₂ are scaled to follow emitter-specific fossil CO₂ per capita emissions based on current pledges. Naturally, the precise scientific framing—e.g., regarding considered time periods, GHGs, and emission allocations—strongly influences the obtained relative contributions of individual emitters to the overall warming^{10,11}.

Results

From emissions to spatially resolved temperature statistics.

Yearly global anthropogenic emissions of Kyoto GHGs have been rising since pre-industrial times before their projected slow decline in the 2020s (Fig. 1a). The increase throughout the IPCC period is mostly caused by the top five emitters, who are set to be responsible for 52% of the total emissions during the IPCC period and 53% during the Paris period under currently pledged NDCs. In both time periods, China is the largest emitter followed by the US, and Russia emits the least of the five. EU-27's total emissions exceed India's for the IPCC period but no longer for the Paris period. Overall, the individual emitters' emission trends throughout the two time periods differ starkly.

We employ a chain of ESM emulators to translate historical and near-term future GHG and aerosol emissions (all considered gases and aerosols are listed in Methods) into yearly local temperature change statistics distributions (Fig. 1). First, time series of historically-constrained, probabilistic forced global mean temperature change

(Δ GMT) are derived from the emissions with the reduced-complexity energy-balance climate model emulator MAGICC^{16,17} (Fig. 1b). This probabilistic set of Δ GMT time series accounts for uncertainty in the Δ GMT response to anthropogenic emissions and the warming is reported with respect to the pre-industrial time period. Subsequently, the Δ GMT time series are converted into spatially resolved yearly land temperature change field time series with the statistical ESM emulator MESMER¹⁸. In this step, two additional sources of uncertainty are accounted for: uncertainty in the regional temperature response to a specific Δ GMT and uncertainty from natural internal climate variability. Due to the computational efficiency of the emulator chain, millions of temperature change field time series can be generated. This allows for reliable estimates of grid-cell-level statistics for any given year, as illustrated for changes in the probability for extreme hot years in a spatially resolved manner for 2030 and with individual time series highlighting the role of the top five emitters for the occurrence of extreme hot years in their own territories (Fig. 1c). Here, an extreme hot year is defined at every grid cell as a 1-in-100-years hot year in pre-industrial climate at that grid cell (i.e., a hot year with a 1% probability of occurrence or exceedance in any year in pre-industrial climate conditions). Both, the MAGICC and the MESMER emulator are calibrated to produce Coupled Model Intercomparison Project Phase 5 (CMIP5¹⁹) ESM consistent temperature change time series and MAGICC additionally takes observational constraints into account. In the supplementary information, it is qualitatively shown that our emulator chain nicely captures the observed warming in the major emitters' territories (Fig. S1).

Country-level warming and probability for extreme hot years.

The impacts of global emissions on median local temperatures are spatially diverse (Fig. 2a) with the fastest warming occurring in the northern high latitudes, due to the Arctic amplification²⁰.

The number of countries surpassing a given warming threshold can be quantified for any Δ GMT value (Fig. 2c). For example, under current NDC pledges, median Δ GMT would reach 1.4 °C in 2030, which leads to 78% (likely range: 19–97%) of all countries experiencing a country-level median warming of more than 1.5 °C by 2030. Here, IPCC calibrated language²¹ is used and the likely range thus refers to the percentage of countries exceeding 1.5 °C in the 17th–83rd percentile range of their median regional warming distribution. Deducting the emissions of the top five during the Paris period, this percentage of countries is reduced to 30% (2–81%) (Fig. 2c). Without their emissions over the full IPCC period, only 2% (0–15%) of all countries would experience more than 1.5 °C country-level warming in 2030. The large spread in the likely range can be explained by the fact that countries cross this temperature threshold during a rather narrow median Δ GMT window. Hence, inter-ESM differences in the regional response to Δ GMT and differences between the median and the actual Δ GMT have a large impact on the percentage of countries above a warming threshold. Note that individual countries surpass a given warming threshold before Δ GMT does, because land is warming faster than oceans, due to the land-sea warming contrast associated with limited water supply on land^{22,23}.

The increase in extreme hot years is also spatially diverse with tropical Africa being the most severely affected region (Fig. 2b). Due to its low natural year-to-year variability²⁴, even the comparably small shift towards warmer temperatures experienced by tropical Africa (Fig. 2a) results in a sharp increase in extreme hot years (Fig. 2b).

Under currently pledged NDCs, extreme hot years are expected to occur at least every second year (probability for hot year \geq 50%) in 92% of all countries (likely range: 72–100%) by 2030 (Fig. 2d).

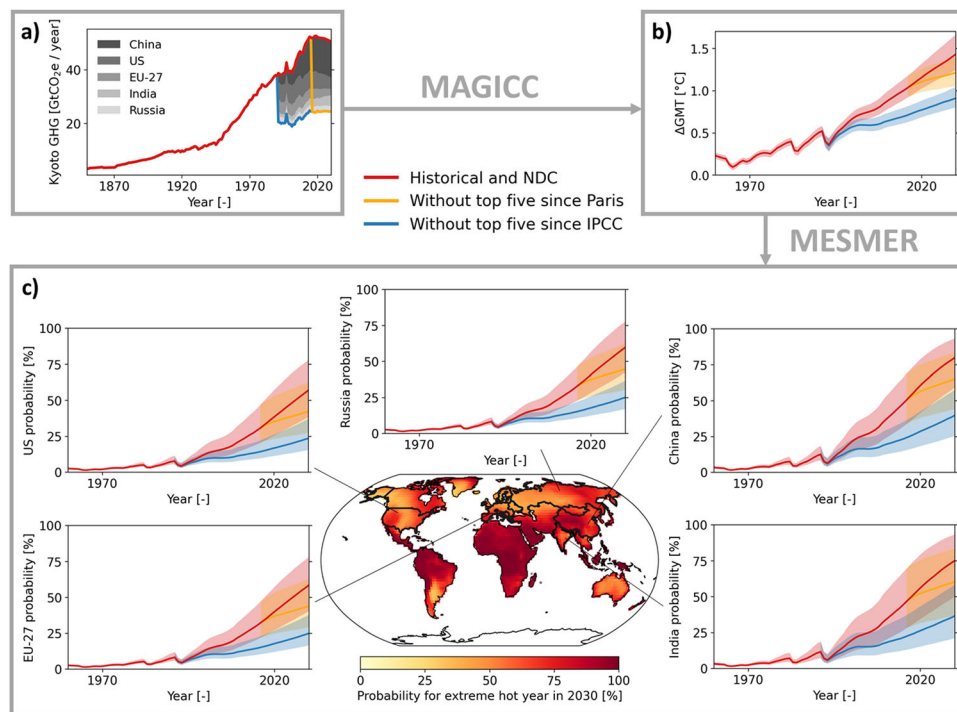


Fig. 1 From emissions to spatially resolved temperature statistics for three scenarios. **a** The reference scenario contains historical global anthropogenic GHG and aerosol emissions and Paris Agreement NDC pledges until 2030. Two hypothetical emission scenarios branch off after the first IPCC report (1991) and after the Paris Agreement (2016) respectively. In those scenarios, the Kyoto GHG emissions of the top five largest emitters—China, US, EU-27, India, and Russia—are removed from the total emissions. All considered types of emissions are listed in Methods. **b** The emissions time series are translated into a probabilistic set of Δ GMT time series relative to pre-industrial levels (1850–1900) with the MAGICC emulator^{16,17}. Here, median Δ GMT is shown with a solid line and the likely range (66% uncertainty range, i.e., 17th–83rd percentile, according to IPCC calibrated language²¹) in shading. **c** The Δ GMT time series are used to create large ensembles of land temperature change field time series with the MESMER emulator¹⁸. The map and the time series depict the probability for an extreme hot year (i.e., a year as warm as that it occurred only about once every 100 years in pre-industrial climate at the grid cell at hand). The map shows the median probability in 2030 and the time series depict the median and the likely range for a typical grid cell within the territory of each of the five largest emitters. The typical grid-cell values are obtained by taking the land-area-weighted average of the individual percentiles across each emitter’s territory.

Without emissions from the top five emitters during the Paris period it would be 77% (53–96%) of all countries instead and without their emissions throughout the IPCC period, this number would further sink to 46% (13–69%).

Per capita scenarios. Per capita emissions provide a complementary perspective to illustrate climate change responsibility. Here, we investigate per capita scenarios in which the whole globe follows per capita fossil CO₂ emissions of each of the major five emitters since the Paris Agreement (Supplementary Fig. S2) and visualise the associated warming in 2030 compared to projected warming under currently pledged global NDCs (Fig. 3). Four of the five top emitters have larger per capita emissions than the global average under their Paris Agreement commitments and would thus be even more severely affected by climate change if the whole world were to emit like them. The US is the largest per capita emitter, followed by Russia, China, EU-27, and finally India.

If global per capita emissions followed the US per capita emissions during the 15 years of the Paris period (2016–2030) alone, Δ GMT would already amount to 1.8 °C (likely range 1.6–2.2 °C) in 2030 which is 0.4 °C more than what is expected under NDC pledges and 0.5 °C more than if everyone followed India’s per capita emissions instead (Fig. 3a). The US scenario would lead to 2.5 °C (2.0–3.1 °C) of warming in the US themselves instead of 1.9 °C (1.5–2.4 °C) under NDC pledges (Fig. 3b) and globally 75% (16–96%) of countries would have

surpassed 2 °C of median warming by 2030 instead of 11% (1–61%) (Fig. 3c). In the India scenario, on the other hand, India’s warming would be reduced to 1.5 °C (1.1–1.8 °C) instead of 1.6 °C (1.3–2.0 °C) (Fig. 3b) and globally only 4% (0–25%) of countries would have surpassed 2 °C of median warming (Fig. 3c). However, also with India’s yearly per capita emissions, the world would continue to warm, albeit at a lower rate. Only moving towards a fully decarbonised society can eventually stop human-induced climate change²⁵.

For completeness, we additionally provide the same per capita figures for the IPCC period in the supplementary information (Figs. S3 and S4).

Discussion

Climate model emulators are simplified but useful tools to rapidly quantify regional warming associated with different GHG and aerosol emission pathways. A diverse range of alternative scenarios can be easily explored, making it possible to highlight the role of single country-level emitters and their emission choices, a task which is too computationally expensive for state-of-the-art ESMs. The obtained quantitative results naturally depend on how emissions are allocated to different countries, which emulators are employed, and how the emulators are calibrated. But regardless of specific allocation and emulator choices, our results reveal that there is a clear country-level warming signal attributable to the major emitters in near-term projections, which reinforces the need for and the immediate benefit of rapid emission reductions

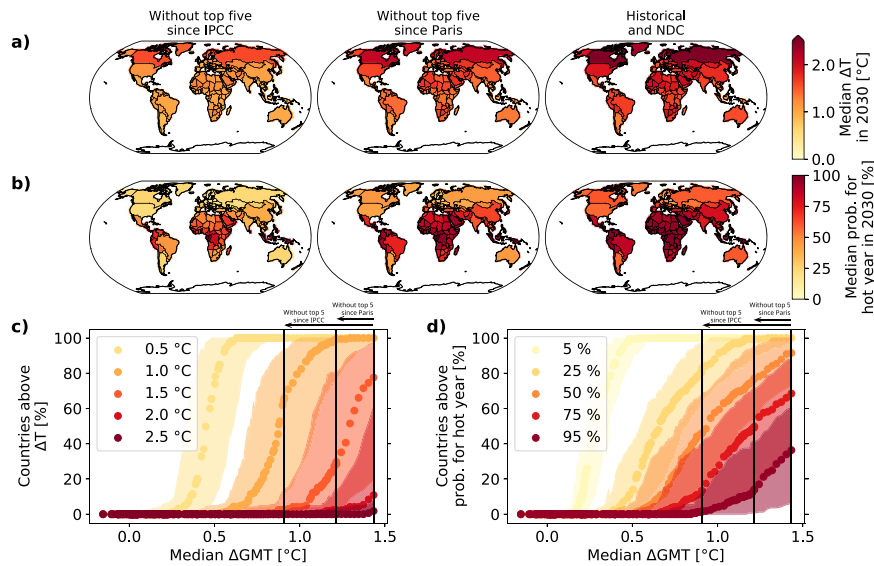


Fig. 2 Country-level median warming and probability for an extreme hot year in 2030 and as a function of median ΔGMT. **a** Map of the median of the 2030 country-level median warming (ΔT) distribution without emissions of the top five emitters during the IPCC period, without emissions of the top five emitters during the Paris period, and under current NDC pledges. **b** Same as **a** but for probability for an extreme hot year to occur instead of median warming. **c** Percentage of countries above selected country-level warming thresholds for different median warming distribution percentiles as a function of median ΔGMT. The dotted lines show the results for the median and the shading the results for the likely range of the country-level median warming distribution. The vertical black lines mark median ΔGMT in 2030 in each of the three scenarios. The results from all three emission scenarios are pooled together in this panel. **d** Same as **c** but for probability for an extreme hot year to occur instead of median warming.

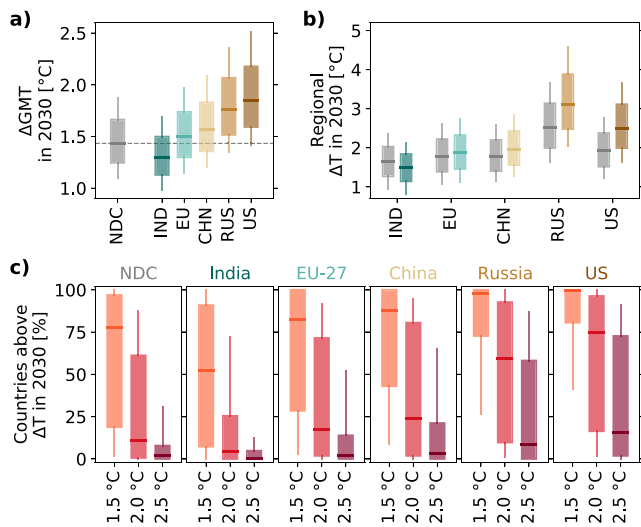


Fig. 3 Median warming in 2030 under historical emissions and currently pledged NDCs and for illustrative per capita scenarios in which the whole world emits fossil CO₂ per capita like the top five emitters during the Paris period. **a** ΔGMT distribution for each scenario. **b** Regional median warming distributions for the top five emitters. For each region, the median warming distribution in the NDC scenario and in the per capita scenario are shown. **c** Percentage of countries above a set of country-level warming thresholds for different median warming distribution percentiles for each scenario. The box-plots indicate the median (line), the likely range (box), and the 5th–95th percentile (whiskers).

by these emitters. Thereby, northern high latitude countries could profit the most in terms of avoided median warming and tropical Africa in terms of avoided frequency of hot extremes.

Overall, we find that the top five emitters—China, US, EU-27, India, and Russia—are playing a major role in driving global and regional warming and are increasing the probability for extreme

hot years, both since the first IPCC report of 1990 and even only since the Paris Agreement of 2015. In the context of their current Paris Agreement emissions pledges, the US, Russia, China, and EU-27 would experience even more severe warming by 2030 if the whole world were to follow the same per capita fossil CO₂ emissions as them.

Identifying the warming implications of commitments of individual countries can be a crucial element to increase transparency in the assessment of countries’ commitments. Under the Paris Agreement, each country is required to regularly update its NDC. Beyond NDCs, the ambition reflected in the long-term strategies further affects the prospects for limiting global warming and bringing the aims of the Paris Agreement within closer reach²⁶. What has been brought forward in new and updated NDCs ahead of COP26—the 26th United Nations Climate Change Conference—in November 2021, is however still insufficient to achieve the goals of the Paris Agreement²⁷. A continued global momentum towards substantial improvements in countries’ 2030 ambition is required to get the world on a Paris Agreement compatible track²⁶. The Glasgow Climate Pact agreed at COP26 explicitly calls on “Parties to revisit and strengthen the 2030 targets in their nationally determined contributions as necessary to align with the Paris Agreement temperature goal by the end of 2022”²⁸. None of the top five emitters currently has an NDC aligned with the 1.5 °C temperature limit of the Paris Agreement²⁹ and their response to the COP26 outcome will be decisive in terms of the global emission trajectory up to 2030. Our results highlight the direct benefits of increased mitigation ambition by the top five emitters for not just less median warming but also a slower emergence of hot extremes already over the next decade. However, this does not imply that smaller emitters do not bear responsibility to increase their commitments. Per capita emission scenarios can be explored for any country and may serve as an intuitive tool to communicate the importance of single countries and their emission choices in driving climate change. This could especially help motivate small countries with large per capita emissions, such as Switzerland and similar-size

countries, to pursue more stringent mitigation efforts, which are urgently needed to meet the Paris Agreement goals^{26,30}. Hence, the presented approach has the potential to support all countries in making evidence-based emission reduction decisions while accounting for different responsibility perspectives.

Methods

Emission scenarios. Two different emission scenario designs are applied in this study, one covering actual past (historical) and planned future (NDC) emission pathways and the other per capita emission pathways.

The historical and NDC emission pathways follow the methodological approach introduced by Nauels et al.¹⁴ which accounts for all Kyoto GHGs (CO₂, CH₄, N₂O, hydrofluorocarbons (HFCs), perfluorocarbons (PFCs) and sulphurhexafluoride (SF₆)) as well as additional non-Kyoto GHGs and aerosols (black carbon (BC), carbon monoxide (CO), ammonium (NH₃), non-CH₄ volatile organic compounds (NMVOCs), nitrates (NO_x), organic carbon (OC), and sulfate aerosol (SO_x)). In this study, historical GHG emissions are inferred from historical Coupled Model Intercomparison Project Phase 6 GHG concentrations^{31,32} until 2014 and extended with PRIMAP-hist emission trends until 2019^{33,34}. These estimates are then combined with pledged NDC emissions until 2030 derived by the Climate Action Tracker consortium^{35,36}, which assesses communicated emission reduction commitments and clarifications provided by governments to construct the pathways. The pledged 2030 emission levels presented here capture the highest plausible emission reductions resulting from the pledged targets. To study the contribution of the five largest emitters to human-induced climate change for two different time periods, additional scenarios are generated, in which fossil CO₂ and the other Kyoto GHG emissions of the top five emitters are removed, whereas non-Kyoto GHGs, land-use CO₂, and aerosols remain untouched (details in Nauels et al.¹⁴). The first time period starts in 1991, after the publication of the first IPCC assessment report, and the second one in 2016, after the Paris Agreement was adopted. Both time periods end in 2030 and thus cover the full time period for which NDC pledges exist. Production emissions are allocated to the country in which the goods are produced in and neither international shipping nor aviation are considered. Note that while Nauels et al.¹⁴ removed the emissions from each of the top five emitters individually, we remove emissions from all five emitters at once, since the collective contribution of the top five emitters is investigated in this study.

The per capita emission pathways serve to investigate the effect of applying different country per capita emission at the global scale for the same two time periods, the IPCC and the Paris period. For these pathways, the focus is set on the contributions of the dominant GHG fossil CO₂ and thus, only fossil CO₂ emissions are manipulated while other GHGs and aerosols—some of which co-emitted with CO₂, others not³⁷—are not modified. This focus is chosen to avoid misleading results due to unclear country-level reporting of land-use CO₂ and non-CO₂ gases as well as temporarily inflated short-term warming when upscaling country-level per capita emissions of potent short-lived GHGs to the global level. Annual emitter-specific fossil CO₂ per capita emissions are derived based on the emitter's fossil CO₂ emission time series described above and its annual population data presented by the European Commission³⁸, using moderate population projections based on the middle-of-the-road Shared Socioeconomic Pathway 2. Per capita fossil CO₂ emission pathways for the individual major emitters are then upscaled to the global scale by multiplication with the global population projections until 2030.

This study does not resolve the temporary GHG emission reductions due to the COVID-19 pandemic³⁹, as the temperature implications of these changes have been assessed to be negligible⁴⁰.

Forced global mean temperature change emulations. MAGICC model version 6.16 is used to produce ΔGMT time series from the emission pathways described above. For every emission pathway, a probabilistic set of ΔGMT projections is generated consisting of a historically-constrained ensemble of 600 runs based on a Metropolis–Hastings Markov Chain Monte Carlo approach¹⁷. For the probabilistic ensemble, the MAGICC configuration parameters are defined to capture the IPCC fifth assessment report equilibrium climate sensitivity likely range of 1.5–4.5 °C (central estimate: 3.0 °C)^{41,42} and carbon-cycle uncertainties⁴³. Note that we solely consider ΔGMT results from the MAGICC emulator here and thus do not account for this emulator's structural uncertainties⁴⁴.

Local land temperature change emulations. The statistical ESM emulator MESMER¹⁸ version 0.8.2 is used to translate MAGICC's ΔGMT estimates into land temperature change field time series, excluding Antarctica, following the approach presented by Beusch et al.⁴⁵. Here, grid cells which are covered by less than 2/3 by ocean, are considered to be land grid cells. The ocean fraction of each grid cell is determined with the land-sea mask of the regionmask package version 0.6.2⁴⁶.

Within MESMER^{18,45}, local warming T for a specific ESM m at every grid cell s and time t consists of a grid-cell-level forced response term T^{fr} and a superimposed additive grid-cell-level internal climate variability term T^{iv} , and can thus be written

as:

$$T_{m,s,t} = T_{m,s,t}^{fr} + T_{m,s,t}^{iv}. \quad (1)$$

Following Beusch et al.⁴⁵, MESMER is calibrated using simulations¹⁹ of the historical time period (1870–2005) as well as all available Representative Concentration Pathways (2006–2100)⁴⁷ for 40 individual CMIP5 ESMs (listed in Table A1 of Beusch et al.¹⁸) on a common 2.5° × 2.5° spatial grid. To emulate emission scenarios which are not available during calibration, estimates of forced global mean warming for these scenarios are needed, since $T_{m,s,t}^{fr}$ is a linear function of the ESM's forced global warming $T_{m,t}^{glob,fr}$ (while $T_{m,s,t}^{iv}$ is an independent stochastic term)⁴⁵. In this study, MAGICC's probabilistic ΔGMT forced global warming estimates are used as $T_{m,t}^{glob,fr}$ estimates in combination with each of the 40 sets of ESM-specific MESMER calibrations to produce globally-constrained probabilistic $T_{s,t}$ warming projections which sample CMIP5 inter-ESM differences in both forced response to global warming and internal climate variability. Thus, it is assumed that global and regional performance of individual ESMs are sufficiently decoupled to allow substituting ESM-specific forced global warming with MAGICC's constrained probabilistic forced global warming, an assumption which has been validated by Beusch et al.⁴⁸. Since forced global warming is the only predictor MESMER employs to create T emulations, the local climate effects of short lived climate forcers^{12,15,49}, in particular aerosols, are not captured in our analysis. As outlined above, aerosol emissions are kept unchanged in our different emission scenarios.

To create the emulations for this study, for each of the 40 ESMs, 600 T^{fr} field time series are created by combining MESMER's local trend parameters with MAGICC's ΔGMT time series. In addition, 6000 T^{iv} field time series realisations are generated for each ESM. Finally, ESM-specific full emulations are created by combining each T^{fr} field time series with every T^{iv} field time series, resulting in 600 (T^{fr} samples) × 6000 (T^{iv} realisations) = 3,600,000 T emulations per ESM and thus in 40 (ESMs) × 3,600,000 (T emulations per ESM) = 144,000,000 T emulations per emission scenario. As with the ΔGMT emulator, we use a single local temperature change emulator here and thus do not account for the emulator's structural uncertainties.

Grid-cell-level statistics. Two types of grid-cell-level statistics are computed in this study, the median warming ΔT and the probability for an extreme hot year p .

To estimate median warming ΔT, we exploit the fact that within MESMER, local warming T consists of a forced response term T^{fr} and an additive internal climate variability term T^{iv} (Equation (1)). Since the climate variability realisations are drawn from a Gaussian distribution with mean 0¹⁸, the median warming of each emulation is by definition the T^{fr} field time series itself. Thus, we have distribution of 600 (T^{fr} samples per ESM and scenario) × 40 (ESMs) = 24,000 median warming estimates available for each scenario.

The probability for an extreme hot year p is a function of both the forced response to global warming (T^{fr}) and the internal climate variability (T^{iv}). Within a sufficiently large single ESM initial-condition ensemble⁵⁰, which samples climate variability around the ESM's forced climate response, the probability for an extreme hot year can be estimated for any year for this ESM. Within MESMER, each combination of a single T^{fr} field time series with the 6000 T^{iv} field time series can be regarded as an approximation of such an initial-condition ensemble which contains 6000 members. Hence, we have 40 (ESM-specific local trend parameters) × 600 (ΔGMT estimates) = 24,000 MESMER initial-condition ensembles available per emission scenario. Within each MESMER initial-condition ensemble, the probability for an extreme hot year p is determined for every year, leading to a distribution of 24,000 probability values for every year and every grid cell. An extreme hot year is here defined as an exceptionally warm year with a probability p of 1% to occur (or to be exceeded) for any given year in pre-industrial times (1850–1900). Thus, it represents the 0.99 quantile of the pre-industrial warming distribution and it is expected to occur about once every 100 years in pre-industrial climate. To study the development of p over time, we first compute the magnitude of the 0.99 quantile of warming in pre-industrial times $T_{q_{0.99},pi}$ based on 51 (pre-industrial years) × 6000 (emulations) = 306,000 warming values at every grid cell. For every year and every grid cell, we subsequently compute the probability p of a year which is at least as hot as $T_{q_{0.99},pi}$ to occur. For this purpose, the quantile q of $T_{q_{0.99},pi}$ is computed for every year and the associated probability for an extreme hot year p is given by $p = (1 - q) \cdot 100$.

Country-level statistics. In this study, country-level averages represent the typical behaviour of a grid cell in this country, meaning the median warming and the probability for an extreme hot year distributions are first computed for every grid cell individually and subsequently area- and land-fraction-weighted averages are derived for different percentiles.

To obtain the grid-cell cover fractions of individual countries, the regionmask package version 0.6.2⁴⁶ is employed. While there are 177 country masks provided by regionmask, only 165 are considered in this study, because Antarctica is excluded and eleven small island nations do not contain any land grid cell on our 2.5° × 2.5° grid, since their land cover fraction is not large enough to reach the minimum threshold to be considered a land grid cell.

Data availability

The CMIP5 data employed for calibration are available from the public CMIP archive at: <https://esgf-node.llnl.gov/projects/esgf-llnl/>. The stratospheric aerosol optical depth data used for the MESMER calibration are provided by NASA and available at: <https://data.giss.nasa.gov/modelforce/strata/>. The MAGICC output is available via zenodo⁵¹.

Code availability

The code to train MESMER, derive the emulations, and plot the figures is openly available at https://github.com/MESMER-group/Beusch_et_al_CEE_2021_major_emitters_cc_responsibility and is additionally stored on zenodo⁵¹.

Received: 22 April 2021; Accepted: 11 November 2021;

Published online: 06 January 2022

References

- Arrhenius, S. On the influence of carbonic acid in the air upon the temperature of the ground. *Philos. Mag. J. Sci.* **41**, 237–276 (1896).
- Manabe, S. & Wetherald, R. T. The effects of doubling the CO₂ concentration on the climate of a General Circulation Model. *J. Atmos. Sci.* **32**, 3–15 (1975).
- Hansen, J. et al. Climate impact of increasing atmospheric carbon dioxide. *Science* **213**, 957–966 (1981).
- IPCC. Climate Change: The IPCC Scientific Assessment Report Prepared by Working Group I (Cambridge University Press, Cambridge, UK and New York, NY, 1990).
- UNFCCC. Adoption of the Paris Agreement. FCCC/CP/2015/10/Add.1 (2015).
- Bindoff, N. et al. Detection and attribution of climate change: from global to regional. In *Climate Change 2013 the Physical Science Basis: Working Group I Contribution to the Fifth Assessment Report of the Intergovernmental Panel on Climate Change* (eds Stocker, T. et al.) 867–952 (Cambridge University Press, Cambridge, United Kingdom and New York, NY, USA, 2013).
- Stott, P. A. et al. Attribution of extreme weather and climate-related events. *Clim Change* **7**, 23–41 (2016).
- Chen, D. et al. Framing, context, and methods. In *Climate Change 2021: The Physical Science Basis. Contribution of Working Group I to the Sixth Assessment Report of the Intergovernmental Panel on Climate Change* (eds Masson-Delmotte, V. et al.) (2021).
- Meinshausen, M. et al. National post-2020 greenhouse gas targets and diversity-aware leadership. *Nat. Clim. Change* **5**, 1098–1106 (2015).
- Skeie, R. B. et al. Perspective has a strong effect on the calculation of historical contributions to global warming. *Environ. Res. Lett.* **12**, 024022 (2017).
- Otto, F. E., Skeie, R. B., Fuglestad, J. S., Berntsen, T. & Allen, M. R. Assigning historic responsibility for extreme weather events. *Nat. Clim. Change* **7**, 757–759 (2017).
- Persad, G. G. & Caldeira, K. Divergent global-scale temperature effects from identical aerosols emitted in different regions. *Nat. Commun.* **9**, 3289 (2018).
- Lewis, S. C., Perkins-Kirkpatrick, S. E., Althor, G., King, A. D. & Kemp, L. Assessing contributions of major emitters' Paris-era decisions to future temperature extremes. *Geophys. Res. Lett.* **46**, 3936–3943 (2019).
- Nauels, A. et al. Attributing long-term sea-level rise to Paris Agreement emission pledges. *Proc. Natl Acad. Sci. USA* **116**, 23487–23492 (2019).
- Lund, M. T. et al. A continued role of short-lived climate forcers under the Shared Socioeconomic Pathways. *Earth System Dyn.* **11**, 977–993 (2020).
- Meinshausen, M., Raper, S. C. B. & Wigley, T. M. L. Emulating coupled atmosphere-ocean and carbon cycle models with a simpler model, MAGICC6 - Part 1: Model description and calibration. *Atmos. Chem. Phys.* **11**, 1417–1456 (2011).
- Meinshausen, M. et al. Greenhouse-gas emission targets for limiting global warming to 2 °C. *Nature* **458**, 1158–1162 (2009).
- Beusch, L., Gudmundsson, L. & Seneviratne, S. I. Emulating Earth System Model temperatures with MESMER: from global mean temperature trajectories to grid-point level realizations on land. *Earth System Dyn.* **11**, 139–159 (2020).
- Taylor, K. E., Stouffer, R. J. & Meehl, G. A. An overview of CMIP5 and the experiment design. *Bull. Am. Meteorol. Soc.* **93**, 485–498 (2012).
- Serreze, M. C. & Barry, R. G. Processes and impacts of Arctic amplification: a research synthesis. *Global Planet. Change* **77**, 85–96 (2011).
- Mastrandrea, M. D. et al. Guidance note for lead authors of the IPCC fifth assessment report on consistent treatment of uncertainties. Intergovernmental Panel on Climate Change (IPCC). (2010).
- Sutton, R. T., Dong, B. & Gregory, J. M. Land/sea warming ratio in response to climate change: IPCC AR4 model results and comparison with observations. *Geophys. Res. Lett.* **34**, L02701 (2007).
- Seneviratne, S. I., Donat, M. G., Pitman, A. J., Knutti, R. & Wilby, R. L. Allowable CO₂ emissions based on regional and impact-related climate targets. *Nature* **529**, 477–483 (2016).
- Hoegh-Guldberg, O. et al. Impacts of 1.5 °C global warming on natural and human systems. In *Global Warming of 1.5 °C. An IPCC Special Report on the Impacts of Global Warming of 1.5 °C Above Pre-industrial Levels and Related Global Greenhouse Gas Emission Pathways, in the Context of Strengthening the Global Response to the Threat of Climate Change* (eds Masson-Delmotte, V. et al.) 175–311 (2018).
- IPCC. Summary for Policymakers. In *Global Warming of 1.5 °C. An IPCC Special Report on the Impacts of Global Warming of 1.5 °C Above Pre-industrial Levels and Related Global Greenhouse Gas Emission Pathways, in the Context of Strengthening the Global Response to the Threat of Climate Change* (Masson-Delmotte, V. et al. eds.) (2018).
- Höhne, N. et al. Wave of net zero emission targets opens window to meeting the Paris Agreement. *Nat. Clim. Change* **11**, 820 (2021).
- UNFCCC. Nationally determined contributions under the Paris Agreement: synthesis report by the secretariat. FCCC/PA/CMA/2021/8 (2021).
- UNFCCC. Glasgow Climate Pact. FCCC/PA/CMA/2021/L.16 (2021).
- CAT. Glasgow's one degree 2030 credibility gap: net zero's lip service to climate action (last accessed 29 November 2021) <https://climateactiontracker.org/press/Glasgows-one-degree-2030-credibility-gap-net-zeros-lip-service-to-climate-action/> (2021).
- Geiges, A. et al. Incremental improvements of 2030 targets insufficient to achieve the Paris Agreement goals. *Earth System Dyn.* **11**, 697–708 (2020).
- Meinshausen, M. et al. Historical greenhouse gas concentrations for climate modelling (CMIP6). *Geosci. Model Dev.* **10**, 2057–2116 (2017).
- Meinshausen, M. et al. The shared socio-economic pathway (SSP) greenhouse gas concentrations and their extensions to 2500. *Geosci. Model Dev.* **13**, 3571–3605 (2020).
- Gütschow, J. et al. The PRIMAP-hist national historical emissions time series. *Earth System Sci. Data* **8**, 571–603 (2016).
- Gütschow, J., Günther, A. & Pflüger, M. The PRIMAP-hist national historical emissions time series v2.3.1 (1750–2019) <https://doi.org/10.5281/zenodo.5494497> (2021).
- CAT. Climate summit momentum: Paris commitments improved warming estimate to 2.4 °C (last accessed 29 October 2021) <https://climateactiontracker.org/publications/global-update-climate-summit-momentum/> (2021).
- CAT. Climate target updates slow as science ramps up need for action (last accessed 29 October 2021) <https://climateactiontracker.org/publications/global-update-september-2021/> (2021).
- Rogelj, J. et al. Air-pollution emission ranges consistent with the representative concentration pathways. *Nat. Clim. Change* **4**, 446–450 (2014).
- European Commission Joint Research Centre. Demographic and Human Capital Scenarios for the 21st Century: 2018 Assessment for 201 Countries (Publications Office of the European Union, Luxembourg, 2018).
- Le Quéré, C. et al. Temporary reduction in daily global CO₂ emissions during the COVID-19 forced confinement. *Nat. Clim. Change* **10**, 647–653 (2020).
- Forster, P. M. et al. Current and future global climate impacts resulting from COVID-19. *Nat. Clim. Change* **10**, 913–919 (2020).
- Rogelj, J., Meinshausen, M. & Knutti, R. Global warming under old and new scenarios using IPCC climate sensitivity range estimates. *Nat. Clim. Change* **2**, 248–253 (2012).
- Rogelj, J., Meinshausen, M., Sedláček, J. & Knutti, R. Implications of potentially lower climate sensitivity on climate projections and policy. *Environ. Res. Lett.* **9**, 031003 (2014).
- Friedlingstein, P. et al. Uncertainties in CMIP5 climate projections due to carbon cycle feedbacks. *J. Climate* **27**, 511–526 (2014).
- Nicholls, Z. et al. Reduced Complexity Model Intercomparison Project Phase 1: introduction and evaluation of global-mean temperature response. *Geosci. Model Dev.* **13**, 5175–5190 (2020).
- Beusch, L. et al. From emission scenarios to spatially resolved projections with a chain of computationally efficient emulators: MAGICC (v7.5.1)—MESMER (v0.8.1) coupling. *Geosci. Model Dev. Discuss.* (2021).
- Hauser, M., Spring, A. & Busecke, J. Regionmask: version 0.6.2 <https://doi.org/10.5281/zenodo.4460457> (2021).
- Moss, R. H. et al. The next generation of scenarios for climate change research and assessment. *Nature* **463**, 747–756 (2010).
- Beusch, L., Gudmundsson, L. & Seneviratne, S. I. Crossbreeding CMIP6 Earth System Models with an emulator for regionally optimized land temperature projections. *Geophys. Res. Lett.* **47**, e2019GL086812 (2020).
- Samset, B. H. et al. Climate impacts from a removal of anthropogenic aerosol emissions. *Geophys. Res. Lett.* **45**, 1020–1029 (2018).
- Deser, C. et al. Insights from Earth System Model initial-condition large ensembles and future prospects. *Nat. Clim. Change* **10**, 277–286 (2020).
- Beusch, L. et al. Data and code for the study: “Responsibility of major emitters for country-level warming and extreme hot years” <https://doi.org/10.5281/zenodo.5608196> (2021).

Acknowledgements

We would like to thank the Climate Action Tracker consortium for sharing data on available GHG emission pledges. We acknowledge the World Climate Research Program's Working Group on Coupled Modelling, which is responsible for the Coupled Model Intercomparison Project, and we thank the climate modelling groups (listed in Table A1 of Beusch et al.¹⁸) for producing and making available their model output. Furthermore, we are indebted to Urs Beyerle and Jan Sedláček for pre-processing the CMIP5 data. L.B. acknowledges partial support from SNF grant P1EZP2_195662. S.I.S. acknowledges partial support from the ERC proof-of-concept MESMER-X project. A.N. and C.F.S. acknowledge support from the European Union's Horizon 2020 Research and Innovation Programme under grant agreement number 820829 (CONSTRAIN).

Author contributions

L.B. computed the MESMER emulations, carried out all analyses, and wrote a first draft of the paper. A.N. and J.G. created the emission pathways. A.N. produced the MAGICC runs. L.B., A.N., L.G., C.F.S., and S.I.S. designed the article, based on an initial idea of C.F.S. S.I.S. proposed the per capita scenarios. All authors interpreted the results together and edited the manuscript.

Competing interests

The authors declare no competing interests.

Additional information

Supplementary information The online version contains supplementary material available at <https://doi.org/10.1038/s43247-021-00320-6>.

Correspondence and requests for materials should be addressed to Lea Beusch.

Peer review information *Communications Earth & Environment* thanks Fabio Sferra and the other, anonymous, reviewer(s) for their contribution to the peer review of this work. Primary Handling Editor: Heike Langenberg.

Reprints and permission information is available at <http://www.nature.com/reprints>

Publisher's note Springer Nature remains neutral with regard to jurisdictional claims in published maps and institutional affiliations.



Open Access This article is licensed under a Creative Commons Attribution 4.0 International License, which permits use, sharing, adaptation, distribution and reproduction in any medium or format, as long as you give appropriate credit to the original author(s) and the source, provide a link to the Creative Commons license, and indicate if changes were made. The images or other third party material in this article are included in the article's Creative Commons license, unless indicated otherwise in a credit line to the material. If material is not included in the article's Creative Commons license and your intended use is not permitted by statutory regulation or exceeds the permitted use, you will need to obtain permission directly from the copyright holder. To view a copy of this license, visit <http://creativecommons.org/licenses/by/4.0/>.

© The Author(s) 2022